© 2016. This manuscript version is made available under the CC-BY-NC-ND 4.0 license http://creativecommons.org/licenses/by-nc-nd/4.0/
The published version is available via https://doi.org/10.1016/j.optcom.2016.02.027.

Highly Polarized Emission from a GaN-based Ultraviolet Light-emitting Diode Using a Si-subwavelength Grating on a SiO_2 Underlayer

Yuusuke Takashima*[a], Masato Tanabe[a], Masanobu Haraguchi[a,b], Yoshiki Naoi[a,b]

[a] Graduate School of Advanced Technology and Science, Tokushima University, 2-1 Minami-josanjima Tokushima 770-8506, Japan
[b] Institute of Technology and Science, Tokushima University, 2-1 Minami-josanjima, Tokushima 770-8506, Japan

*Corresponding author.
E-mail: takashima@ee.tokushima-u.ac.jp,
Phone: +81 88 656 7447
Fax: +81 88 656 7447

Abstract

The polarization characteristics of a 370 nm GaN-based ultraviolet light-emitting diode (UV-LED) were controlled by a subwavelength grating (SWG) on a low-refractive-index SiO_2 underlayer inserted between the SWG and LED surface. Highly polarized UV emission was demonstrated by utilizing the Bloch eigenmode resonance in the SWG structure for the two orthogonal polarization states. The polarization ratio of the emission reached 16:1, which is the highest reported to date for direct emission from a GaN-based UV-LED. The decrease in UV emission was also prevented by suppressing the diffracted plane wave and by increasing the amplitude of the wave incident onto the SWG structure; this increase was achieved by taking advantage of the low refractive index of SiO_2.

Keywords: Polarization, subwavelength, ultraviolet, light-emitting diode, nitride

Highlights:

- GaN-based UV-LED was designed with Si subwavelength grating over a SiO_2 underlayer.
- Highly polarized emission demonstrated experimentally with Si-SWG/SiO_2 structure.
- Polarization ratio was as high as 16:1 at ~370 nm with low loss in intensity.
- P-polarized EL intensity was 1.2 times higher than that of a diode without the SWG.

1 Introduction

Highly polarized GaN-based ultraviolet-light-emitting diodes (UV-LEDs) have unique applications. For example, irradiation by a linearly polarized UV wave can induce optical anisotropy in photoreactive polymers, whereas visible irradiation cannot [1]. This property is particularly suitable for achieving the alignment of liquid crystals in the absence of rubbing and patternable processes [1, 2]. Most such applications require the use of highly polarized UV emission, without a significant decrease in emission intensity.

A polarizing plate, composed of an iodine-doped polymer, is generally used to control the polarization of the LED emission. The transmittance through such a filter is very low, especially in the UV region (~30% at 360 nm), because most photons are absorbed in the polymer. Several groups have recently fabricated polarized nitride-based LEDs using semi- or non-polar crystals, photonic crystals, and wire grids [3-12]. You et al. found that the electroluminescence (EL) spectra in the visible region from *m*-plane InGaN/GaN LEDs have a polarization ratio (defined as the intensity ratio of the two orthogonal polarizations) of 7.7 at 505 nm [3]. The polarized photoluminescence (PL) spectra from *m*-plane InGaN/GaN were observed to have a polarization ratio of 3.8 at ~440 nm [4]. Matioli et al. reported that a polarization ratio of 16.7 and a light-extraction efficiency of 80% were achieved at 465 nm for an *m*-plane GaN-based LED with photonic crystal structure [5]. Wang et al. obtained highly polarized PL spectra from an InGaN LED with a multilayer wire-grid structure [9]. The polarization ratio attained was 100:1 at 530 nm.

Highly polarized in-plane emission in the UV region has been reported for LEDs. Kolbe et al. demonstrated polarized in-plane emission at various UV wavelengths from an InGaN/AlInGaN LED grown on a *c*-plane sapphire substrate [10]. They observed the in-plane emissions from the UV-LED to have a polarization ratio of 5:1 at 380 nm. Durnev and Karpov reported the emission characteristics of a UV-LED with an InGaN/GaN quantum well (QW) and an InGaN/AlGaN QW [11]. The in-plane polarization ratio was 3.7 at 380 nm. Schade et al. performed PL measurements of the polarized emission from a strained InGaN QW grown on a semipolar GaN substrate [12]. However, a high-quality freestanding GaN substrate, which is very expensive, is required to reduce the dislocation density in the non- or semi-polar QWs [13].

Highly polarized UV emission without loss of emission intensity can be achieved by using a high-contrast sub-wavelength grating (SWG) above a *c*-plane UV-LED [14-27]. The period of the SWG is shorter than the incident wavelength. Bloch eigenmodes are formed in the SWG structure owing to a periodic refractive-index

distribution, and these Bloch modes wave can interact with the incident wave. In the SWG, the coupling between the incident plane wave and the higher order diffracted plane wave is suppressed because of the subwavelength period. If the Bloch eigenmodes are in antiphase and cancel each other, the intensity of the transmitted wave decreases. This interaction strongly depends on the polarization states of the Bloch eigenmode because of different boundary conditions for orthogonal polarizations. Therefore, polarization selectivity can be obtained [14, 16-21, 23-27]. The transmittance through the SWG is determined by the interaction between the Bloch eigenmode wave and the incident wave in the SWG structure; therefore, the transmittance is not directly connected to the absorption properties of the material. High transmittance can be achieved by exploiting the above interaction despite the large absorption coefficient of the material, which is directly related to macroscopic photon absorption.

In a previous study, we reported polarized emission from a GaN-based UV-LED grown on a *c*-plane sapphire substrate using an SWG structured on the surface [26]. The polarization ratio of the emission from the *c*-plane UV-LED was approximately 4:1 at 360 nm. We also noted that the incident plane wave strongly coupled with +1 and −1 diffraction order plane waves, outgoing from the SWG, at the interface between the SWG and the high-refractive-index semiconductor of the LED, e.g., GaN. This is because the subwavelength condition is not satisfied at the interface between the p-GaN and the grating, owing to the much shorter wavelength in the semiconductor than in air (i.e., the wavelength in the semiconductor < the grating period). The energy of the incident wave is dispersed by the diffracted plane wave, so the polarization ratio and the transmittance through the SWG are decreased [26].

In the present study, we sought to develop a highly polarized *c*-plane UV-LED while avoiding a decrease in its emission intensity by utilizing an SWG with a low-refractive-index underlayer (SiO_2) above the LED, as shown in Fig. 1. We used Si as the high-refractive-index material of the SWG because Si-SWG has a high refractive index compared to the surrounding material [16-21]. A SiO_2 underlayer was inserted between the Si-SWG and the top of the LED to satisfy the subwavelength condition at the interface between GaN and Si-SWG. An increase in the emission intensity is also expected upon insertion of a SiO_2 underlayer for the following reason. For a planar GaN-based LED, the escape cone is limited by the total internal reflection, namely the refractive index contrast, at the surface (GaN/air interface). In our LED, the escape cone is broader than that of a planar LED because of the presence of the SiO_2 underlayer; in other words, the contrast in the refractive index at the SiO_2/GaN interface is less than that at the GaN/Air interface. This allows more energy of the incident wave to reach the

SWG region. The Bloch eigenmode wave inside the SWG interacts with the incident wave, and the energy of the wave is emitted into the air. The Bloch eigenmode wave can also interact with the incident wave when the incident angle is greater than the critical angle. Thus, we expected an increase of the emission into the air compared to the case of a planar LED.

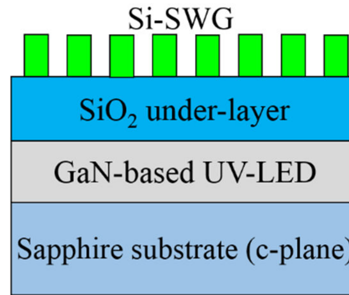

Fig. 1 Schematic diagram of a UV-LED with a Si-SWG/SiO_2 underlayer structure. The SiO_2 underlayer is deposited on the GaN-based UV-LED surface, and the Si-SWG is arranged on the SiO_2 underlayer.

2 Theoretical investigation

The interaction between the Bloch eigenmode wave and the incident wave dominates the polarization characteristics of the SWG. Previous studies reported that the grating period and filling factor (defined as the ratio of the grating bar width to the period) determine the number of the order of the Bloch eigenmode, and the grating thickness is related to the phase of the mode [17-20, 21, 24, 26, 27]. After referring to these publications, we investigated the electromagnetic-field distribution using the finite-difference time domain (FDTD) method to design the SWG for the polarization control of the UV-LED. The design criterion was to achieve both high transmittance and a high polarization ratio at 370 nm.

Figure 2 shows the schematic model for the calculation of the electromagnetic field distribution using the FDTD method. In this model, a SiO_2 underlayer is deposited on the p-type GaN of the top of the LED. Subsequently, a Si-SWG is fabricated on the SiO_2 underlayer. For the model without the SiO_2 underlayer, the Si-SWG is directly arranged on the p-type GaN. The refractive-index values at 370 nm for SiO_2 (n_{SiO2} = 1.487 + 0i), p-type GaN (n_{GaN} = 2.46 + 0.065i), and Si (n_{Si} = 3.963 + 2.595i) were taken from the literature [28-30]. The thickness of the SiO_2 layer (L) was set to 200 nm. We assumed that the Si-SWG has an infinite length along the y-direction. A perfectly

matched layer (PML) and periodic boundary conditions (PBC) were used in the z and x directions, respectively. The number of PML layer was 20. The calculation region was defined as the region surrounded by each boundary shown in Fig. 2. The vertical and lateral size of the calculation region were 920 nm and 820 nm, respectively. The calculation region was divided into 2 nm $\times$ 2 nm rectangle cell. The time step in this calculation was 0.47 $\times$ 10^{-18} s. The incident plane wave with a wavelength of 370 nm was either p- or s-polarized. The direction of the electric-field vector in the case of s- or p-polarization is parallel or perpendicular, respectively, to that of the grating stripe. The reason why we used the monochromatic wavelength of 370 nm in this simulation is that excellent broadband polarization selectivity can be obtained in the high contrast SWG, and uniform polarization characteristics over the LED emission spectrum can be expected [16-25]. The incident wave propagates from p-type GaN on the UV-LED surface to air. The transmittance from p-GaN to air was calculated at the observation plane in Fig.2. The distance (d) between the observation plane and SiO_2 layer was 540nm. The grating thickness was varied, while keeping the grating period and width of the Si-SWG fixed at Λ = 205 nm and w = 100 nm.

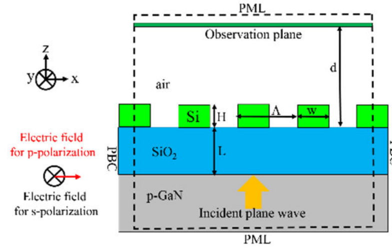

Fig. 2 Schematic of the FDTD numerical model.

Figure 3 shows that when the grating thickness H increases, the transmittance for the p-polarized wave oscillates in both cases, i.e., with and without the SiO_2 underlayer. For H = 10–80 nm, the transmittance without the SiO_2 underlayer is higher than that with SiO_2, but when H is greater than 80 nm, the transmittance with SiO_2 is higher than that without SiO_2. However, the transmittance for the s-polarized wave simply decreases with the increase of H. The transmittance for s-polarization is considerably smaller than that for p-polarization. Also, the transmittance through the SWG with the SiO_2 underlayer is lower than that without the layer, which results in high polarization selectivity. The calculation indicates that both a high polarization ratio and high transmittance can be achieved at H = 90 nm. A high polarization ratio of 57:1 (the ratio of transmittance for p-polarization to that for s-polarization) is expected, with the

transmittance for p-polarization through the structure being maintained at 43%. The high polarization selectivity and high transmittance in the case of the p-polarized wave cannot be explained by the excitation of surface plasmons, because the surface plasmon excitation condition is not satisfied in our structure [31]. To clarify the origin of the high polarization selectivity and the drastic increase of transmittance for the p-polarized wave, the magnetic-field distributions at H = 90 nm are shown in Fig. 4, where the magnetic-field intensity is normalized by the intensity of the light-source. The magnetic-field distributions for the s-polarized wave in Fig. 4 (a) and (c) indicate that the Bloch eigenmodes cancel each other at the interface between the Si-SWG and air, and the transmitted field intensities are very low. In contrast, we found that the Bloch eigenmodes for p-polarization reinforce each other at the interface, and the intensity of the transmitted field is larger than that of the s-polarized field as shown in Fig. 4 (b) and (d). The p- and s-polarized magnetic fields for the UV-LED without the SiO_2 underlayer also indicate that the wavefront is not planar at the interface between the LED surface and the Si-SWG; a part of the incident wave reflects back to generate a diffraction pattern in the GaN, as displayed in Fig. 4 (a) and (b). The coupling between the diffracted plane wave and the incident plane wave affects the energy flow in the SWG, thus leading to deviations in the optical response of the SWG [16-19, 21-24]. For the UV-LED with the SiO_2 underlayer shown in Fig. 4 (c) and (d), the coupling is suppressed because the subwavelength condition is satisfied (namely, the wavelength in SiO_2 > the grating period). The transmitted field intensity in the UV-LED with the SiO_2 underlayer is greater than that without the SiO_2 underlayer, and the SiO_2 underlayer is found to be useful for realizing both high transmittance and a high polarization ratio.

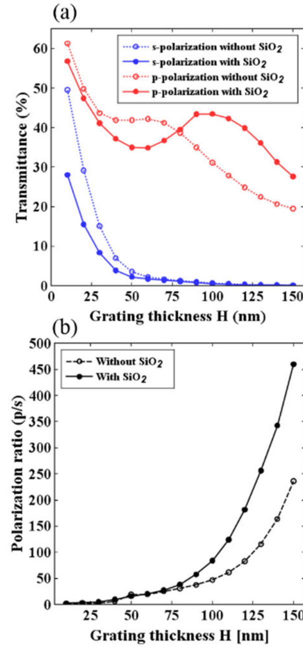

Fig. 3 (a) Transmittance and (b) polarization ratio for the Si-SWG with and without the SiO_2 underlayer as a function of grating thickness H. The values of Λ, w, and L are set to 205 nm, 100 nm, and 200 nm, respectively.

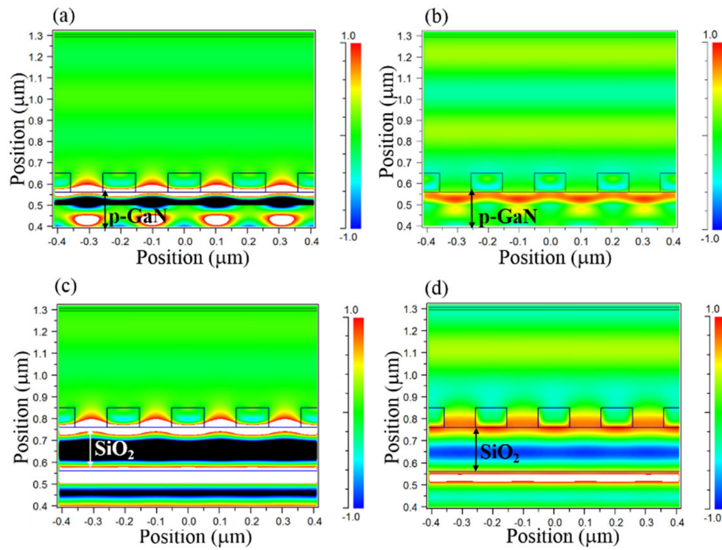

Fig. 4 The distribution of magnetic-field intensity at a given time: (a) s-polarization without the SiO_2 underlayer (b) p-polarization without the SiO_2 underlayer (c) s-polarization with the SiO_2 underlayer (d) p-polarization with the SiO_2 underlayer.

3 Experimental procedure

The designed Si-SWG/SiO_2 structure with Λ = 205 nm, H = 90 nm, and w = 100 nm was fabricated on a GaN-based UV-LED grown on a *c*-plane sapphire substrate by metalorganic chemical vapor deposition method. The LED consisted of undoped GaN, an n-type GaN layer, n-type AlGaN, an AlGaN/GaN quantum well, p-type AlGaN, a p-type GaN layer, and a p-type-contact (Au/Ni: 10 /10 nm). The contact area was 1 mm × 1 mm. A 200-nm-thick SiO_2 film was deposited onto the UV-LED surface by electron-beam evaporation. The grating resist pattern was then fabricated on the SiO_2 layer by electron-beam lithography [26]. A 90-nm-thick Si film was evaporated using an electron beam on the patterned resist, after which the resist was removed. After the SWG fabrication process, we investigated the emission characteristics of the UV-LED. Figure 5 outlines the setup used for EL measurements. The p- and s-polarized EL intensities were measured by rotating a polarizing plate in front of the LED.

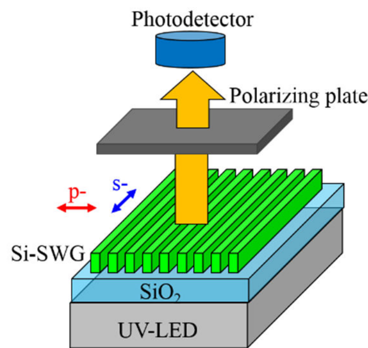

Fig. 5 Schematic diagram of the setup used for EL measurements. The red and blue arrows show the direction of the electric field for the p- and s-polarized waves, respectively.

4 Results and discussion

Figure 6 shows the EL spectra from the UV-LED for a forward current I_F of 20 mA (current density 20mA/mm^2). The emission peak appears at 370 nm. The polarization ratio of the emission from the UV-LED without the SWG structure is nearly 1:1, as

shown in Fig. 6 (a), and the emission is unpolarized. Unpolarized emission along the c-axis is caused by the growth of the GaN active layer on the *c*-plane sapphire substrate. In contrast, the spectra from the UV-LED with a Si-SWG/SiO_2 underlayer structure shows highly polarized emission, as demonstrated in Fig. 6 (b), with a polarization ratio as high as ~16:1 around 370 nm. To the best of our knowledge, this is the highest value obtained for polarized UV-LEDs, and is 4 times the value obtained in our previous study [26]. The origin of this high polarization ratio can be attributed to the suppression of the higher order diffractions at the interface between the LED surface and the SWG, because the subwavelength condition is satisfied by SiO_2 underlayer. The polarization ratio calculated by using the FDTD method is greater than the measured ratio. The experimental polarization ratio is determined not only by the ratio of the transmittance of p- and s- polarization through the SWG structure, but also by many other factors including light absorption in the bulk of LED chip and in the metal contact electrodes, as well as chip geometry. We ignored these factors, because the emission from the LED without the SWG is nearly unpolarized as shown in Fig. 6 (a). We speculated that one source of this discrepancy was the natural surface oxidation of the Si grating. If one considers the 6-nm-thick oxidation layer formed on the Si-SWG surface, the calculated polarization ratio is ~ 17:1, which is in good agreement with the experimental value of the ratio. In addition, the photons emitted from the active layer may reach the SWG at various angles of incidence. We speculated that this might also be another source of disagreement between the experimental and theoretical results. Moreover, the p-polarized luminescence intensity from the present UV-LED is approximately 1.2 times that of the UV-LED without the SWG structure. One important reason for the increased luminescence intensity is that—for the UV-LED with the Si-SWG/SiO_2 structure—the escape angle of the photons at the GaN/SiO_2 interface is than that at the GaN/air interface. Thus, in this case, the additional photons can interact with the Bloch eigenmode within the SWG. We also investigated the influence of the SWG structure on the current-voltage and EL intensity-current characteristics of the UV-LED. The threshold voltage (V_{th}) for the passage of 20 mA current was 4.98 V, and the current-voltage characteristic was almost the same as in the absence of the SWG structure. The magnitude of the EL spectra increased substantially and linearly as the current increased to 50 mA.

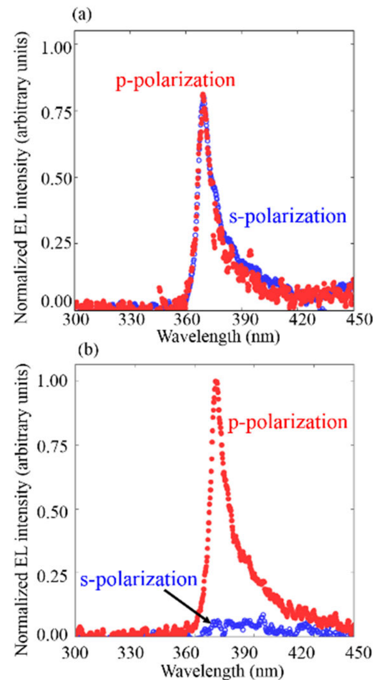

Fig. 6 Normalized EL spectra for a forward current of 20 mA from the UV-LED. (a) Without the Si-SWG/SiO_2 underlayer structure. The peak wavelength of the emission spectra is approximately 370 nm. The filled and open circles indicate p- and s-polarized EL intensity, respectively. The spectra show unpolarized emission. (b) With the Si-SWG/SiO_2 underlayer structure. The spectra show highly polarized emission. The polarization ratio reaches a value of ~16:1 around 370 nm. The intensity of the p-polarization is approximately 1.2 times that without the SWG structure.

5 Summary

In summary, we successfully achieved highly polarized emission from a GaN-based UV-LED without decreasing the EL emission intensity, by using a Si-SWG/SiO_2 underlayer structure. The electromagnetic distribution within the SWG was calculated to optimize the SWG structure for achieving both high transmittance and a high polarization ratio. The results also showed that the SiO_2 underlayer suppresses the diffracted plane wave at the LED surface and is very useful for avoiding a decrease in transmittance. The measured polarization ratio was ~16:1 at 370 nm. The p-polarized EL intensity from the UV-LED with the SWG/SiO_2 underlayer structure was 1.2 times

greater than that from the same device without this structure. These results suggest that the UV-LED with the SWG/SiO_2 underlayer can play an important role in the development of various integrated photonic devices operating in the UV region.

Acknowledgments

We thank Prof. S. Sakai of Tokushima University for the preparation of the UV-LED samples, and also Dr. T. Tomita of Tokushima University for discussions of the measurement results. This work was supported in part by a Grant-in-Aid for Scientific Research (24560377) from the Japan Society for the Promotion of Science.

References

[1] H. Watanabe, N. Miyagawa, S. Takahara, T. Yamaoka, Photo-alignment material with azobenzene-functionalized polymer linked in film, Polym. Adv. Technol. 13 (2002) 558-565.

[2] D.H. Choi, Y.K. Cha, Photo-alignment of low-molecular mass nematic liquid crystals on photoreactive polyimide and polymethacrylate film by irradiation of a linearly polarized UV light, Polym. Bull. 48 (2002) 373-380.

[3] S. You, T. Detchprohm, M. Zhu, W. Hou, E.A. Preble, D. Hanser, T. Paskova, C. Wetzel, Highly polarized green light emitting diode in *m*-axis GaInN/GaN, Appl. Phys. Express 3 (2010) 102103.

[4] T. Koyama, T. Onuma, H. Masui, A. Chakraborty, B.A. Haskell, S. Keller, U.K. Mishra, J.S. Speck, S. Nakamura, S.P. DenBaars, T. Sota, S.F. Chichibu, Prospective emission efficiency and in-plane light polarization of nonpolar *m*-plane $In_xGa_{1-x}N$/GaN blue light emitting diodes fabricated on freestanding GaN substrates, Appl. Phys. Lett. 89 (2006) 091906.

[5] E. Matioli, S. Brinkley, K.M. Kelchner, Y.L. Hu, S. Nakamura, S. DenBaars, J. Speck, C. Weisbuch, High-brightness polarized light-emitting diodes, Nat. Light Sci. Appl. 1 (2012) e22.

[6] C.F. Lai, J.Y. Chi, H.H. Yen, H.C. Kuo, C.H. Chao, H.T. Hsueh, J.F.T. Wang, C.Y. Huang, W.Y. Yeh, Polarized light emission from photonic crystal light-emitting diodes, Appl. Phys. Lett. 92 (2008) 243118.

[7] L. Zhang, J.H. Teng, S.J. Chua, E.A. Fitzgerald, Linearly polarized light emission from InGaN light emitting diode with subwavelength metallic nanograting, Appl. Phys. Lett. 95 (2009) 261110.

[8] M. Ma, D.S. Meyaard, Q. Shan, J. Cho, E.F. Schubert, G.B. Kim, M.H. Kim, C. Sone, Polarized light emission from GaInN light-emitting diodes embedded with subwavelength aluminum wire-grid polarizers, Appl. Phys. Lett. 101 (2012) 061103.
[9] M. Wang, B. Cao, C. Wang, F. Xu, Y. Lou, J. Wang, K. Xu, High linearly polarized light emission from InGaN light-emitting diode with multilayer dielectric/metal wire-grid structure, Appl. Phys. Lett. 105 (2014) 151113.
[10] T. Kolbe, A. Knauer, C. Chua, Z. Yang, V. Kueller, S. Einfeldt, P. Vogt, N.M. Johnson, M. Weyers, M. Kneissl, Effect of temperature and strain on the optical polarization of (In)(Al)GaN ultraviolet light emitting diodes, Appl. Phys. Lett. 99 (2011) 261105.
[11] M.V. Durnev, S.Y. Karpov, Polarization phenomena in light emission from C-plane Al(In)GaN heterostructures, Phys. Status Solidi B 250 (2013) 180-186.
[12] L. Schade, U.T. Schwarz, T. Wernicke, J. Rass, S. Ploch, M. Weyers, M. Kneissl, On the optical polarization properties of semipolar InGaN quantum wells, Appl. Phys. Lett. 99 (2011) 051103.
[13] K.H. Li, Q. Wang, H. P.T. Nguyen, S. Zhao, Z. Mi, Polarization-resolved electroluminescence study of InGaN/GaN dot-in-a-wire light-emitting diodes grown by molecular beam epitaxy, Phys. Status, Solidi A 212 (2015) 941-946.
[14] S.Y. Chou, W. Deng, Subwavelength amorphous silicon transmission gratings and applications in polarizers and waveplates, Appl. Phys. Lett. 67 (1995) 742.
[15] L. Zhuang, S. Schablitsky, R.C. Shi, S.Y. Chou, Fabrication and performance of thin amorphous Si subwavelength transmission grating for controlling vertical cavity surface emitting laser polarization, J. Vac. Sci. Technol. B 14 (1996) 4055-4057.
[16] R. Magnusson, M. Shokooh-Saremi, Physical basis for wideband resonant reflectors, Opt. Express 16 (2008) 3456-3462.
[17] V. Karagodsky, B. Pesala, F.G. Sedgwick, C.J. Chang-Hasnain, Dispersion properties of high-contrast grating hollow-core waveguides, Opt. Lett. 35 (2010) 4099-4101.
[18] Y. Zhou, M.C. Y. Huang, C. Chase, V. Karagodsky, M. Moewe, B. Pesala, F.G. Sedgwick, C.J. Chang-Hasnain, High-index-contrast grating (HCG) and its applications in optoelectronic devices, IEEE J. Sel. Top. Quantum Electron. 15 (2009) 1485-1499.
[19] V. Karagodsky, F.G. Sedwick, C.J. Chang-Hasnain, Theoretical analysis of subwavelength high contrast grating reflectors, Opt. Express 18 (2010) 16973-16988.
[20] C. Chase, Y. Rao, W. Hofmann, and C.J. Chang-Hasnain, 1550 nm high contrast grating VCSEL, Opt. Express 18 (2010) 15461-15466.
[21] C.J. Chang-Hasnain, High-contrast gratings as a new platform for integrated

optoelectronics, Semicond. Sci. Techol. 26 (2011) 014043.
[22] G.G. Kang, I. Vartiainen, B.F. Bai, H. Tuovinen, J. Turunen, Inverse polarizing effect of subwavelength metallic gratings in deep ultraviolet band, Appl. Phys. Lett. 99 (2011) 071103.
[23] T.T. Wu, Y.C. Syu, S.H. Wu, W.T. Chen, T.C. Lu, S.C. Wang, H.P. Chiang, D.P. Tsai, Sub-wavelength GaN-based membrane high contrast grating reflectors, Opt. Express 20 (2012) 20551-20557.
[24] Y. Laaroussi, C. Christyves, F. Genty, N. Fressengeas, L. Cerutti, T. Taliercio, O. Gauthier-Lafaye, P.L. Calmon, B. Reig, J. Jacquet, G. Almuneau, Oxide confinement and high contrast grating mirrors for Mid-infrared VCSELs, Opt. Mater. Express 3 (2013) 1576-1585.
[25] M. Gebski, M. Dems, J. Chen, Q.J. Wang, D.H. Zhang, T. Czyszanowski, The influence of imperfections and absorption on the performance of a GaAs/AlO_x high-contrast grating for monolithic integration with 980 nm GaAs-Based VCSELs, J. Lightwave Technol. 31 (2013) 3853-3858.
[26] Y. Takashima, R. Shimizu, M. Haraguchi, Y. Naoi, Polarized emission characteristics of UV-LED with subwavelength grating, Jpn. J. Appl. Phys. 53 (2014) 072101.
[27] Y. Takashima, R. Shimizu, M. Haraguchi, Y. Naoi, Influence of low-contrast subwavelength grating shape on polarization characteristics of GaN-based light-emitting diode emissions, Opt. Eng. 54 (2015) 067112.
[28] T. Iwanaga, T. Suzuki, S. Yagi, T. Motooka, Optical absorption properties of Mg-doped GaN nanocolumns, J. Appl. Phys. 98 (2005) 104303.
[29] D.T. Pierce, W.E. Spicer, Electronic structure of amorphous Si from photoemission and optical studies, Phys. Rev. B 5 (1972) 3017-3028.
[30] L. Gao, F. Lemarchand, M. Lequime, Exploitation of multiple incidences spectrometric measurements for thin film reverse engineering, Opt. Express 20 (2012) 15734-15751.
[31] L.B. Mashev, E. Popov, E.G. Loewen, Brewster effects for deep metallic gratings, Appl. Opt. 28 (1989) 2538-2541.